ResearchGate

See discussions, stats, and author profiles for this publication at: https://www.researchgate.net/publication/13450054

# Structural and Biological Stability of the Human Interleukin 10 Homodimer †

**ARTICLE** *in* BIOCHEMISTRY · JANUARY 1999

Impact Factor: 3.02 · DOI: 10.1021/bi981555y · Source: PubMed

CITATIONS
35

READS
30

**6 AUTHORS**, INCLUDING:

Nicholas John Murgolo
Merck
**59** PUBLICATIONS **2,778** CITATIONS
SEE PROFILE

Emory H. Braswell
University of Connecticut
**52** PUBLICATIONS **1,422** CITATIONS
SEE PROFILE

Available from: Nicholas John Murgolo
Retrieved on: 01 February 2016

# Structural and Biological Stability of the Human Interleukin 10 Homodimer†

Rosalinda Syto,‡ Nicholas J. Murgolo,‡ Emory H. Braswell,§ Philip Mui,‡,|| Eric Huang,‡,⊥ and William T. Windsor*,‡

*Schering-Plough Research Institute, 2015 Galloping Hill Road, Kenilworth, New Jersey 07033, and National Analytical Ultracentrifugation Facility and Department of Molecular and Cell Biology, The University of Connecticut, Storrs, Connecticut 06269*

*Received June 30, 1998; Revised Manuscript Received September 23, 1998*

ABSTRACT: Human interleukin 10 (huIL-10) is a cytokine that regulates the synthesis of type 1 helper T cell derived cytokines such as $\gamma$-interferon, interleukin 2, and tumor necrosis factor α. The potential immunosuppressive activities of huIL-10 suggest that this protein may be clinically useful for treating autoimmune diseases. Due to the potential clinical value of this cytokine, physicochemical studies have been performed regarding its association state and biological/structural stability. These studies include performing size-exclusion chromatography, chemical cross-linking, equilibrium ultracentrifugation, and circular dichroism spectroscopy. The results indicate huIL-10 is predominantly a noncovalent homodimer at neutral pH and 4 °C for concentrations greater than 0.003 mg/mL (0.08 $\mu$M dimer). An apparent p$K_a$ value of ∼4.8 was calculated for both the pH-dependent subunit dissociation and pH-induced loss in MC/9 biological activity. A temperature analysis revealed a linear relationship between the percent dimer and relative MC/9 activity, thus, these results and the pH-dependent activity results suggest that the huIL-10 dimer is the active species. The GndHCl-induced unfolding of rhuIL-10, monitored by far-UV circular dichroism, revealed a unique biphasic unfolding process which contained both a subunit dissociation process (<1.6 M GndHCl) as well as the unfolding of a highly α-helical monomer intermediate ($[GndHCl]_{1/2}$ = 3.5 M). The monomer intermediates generated with 1.6 M GndHCl or pH 2.5 retained ∼80% and 89% of the α-helical content of the native protein, respectively. Although a soluble and highly helical monomer state can be generated, the observed correlation between unfolding studies and biological activity suggests the dimer is the active species. These results are consistent with both the recent observation that the three-dimensional structure of rhuIL-10 is a 2-fold symmetric homodimer and that a complex between the extracellular domain of the recombinant human IL-10 receptor and IL-10 is consistent with two IL-10 homodimers and four receptors.

Interleukin 10 (IL-10) is a cytokine that was originally identified as a product of the type 2 helper T cell and subsequently shown to be produced by other cell types including B cells and macrophages (*1*−*4*). IL-10 has pleiotropic activities including the ability to inhibit the synthesis of several cytokines produced from type 1 helper T cells such as $\gamma$-interferon, interleukin 2, and tumor necrosis factor α (*4*). Inhibition of these cell-mediated immune response modulators by IL-10 and its suppression of antigen-presenting cell-dependent T cell responses suggest that IL-10 may have immunosuppressive activities which are favorable for treating autoimmune diseases such as allograft rejection and diabetes (*5*−*8*). The protein also displays antiinflammatory activity by inhibiting the monocyte/macrophage production of cytokines such as IL-1α, IL-6, IL-8, granulocyte-macrophage colony-stimulating factor (GM-CSF), granulocyte colony-stimulating factor (G-CSF), and TNFα (*3*, *5*). This activity suggests that IL-10 may be useful for treating clinical situations such as bacterial sepsis (*9*), enterotoxin-induced lethal shock, and rheumatoid arthritis (*5*, *6*, *10*).

The cDNAs of both murine IL-10 (muIL-10) and human IL-10 (huIL-10) (*11*, *12*) code for 178 amino acid long proteins which include a 21 and 18 amino acid signal sequence, respectively (*6*, *13*). The sequence identity between the mature forms of recombinant muIL-10 (157 amino acids, 18 453 Da) and recombinant huIL-10 (160 amino acids, 18 647 Da) is very high, 73%, which for huIL-10 appears to be sufficient to enable it to be biologically active on murine cells, though muIL-10 is inactive on human cells. The biological activity of IL-10 is mediated through its high-affinity binding ($K_d$ ∼50−200 pM) to cell surface receptors (*14*, *15*). The mechanism by which IL-10 induces a biological response is expected to be similar to other cytokines which bind to cell surface membranes and induce the association of two or more receptors. The primary sequence for the murine IL-10 receptor (*15*) has a sequence similar to the class II (interferon-like) cytokine receptor superfamily (*16*). This observation, along with the fact that

† The National Analytical Ultracentrifugation Facility at The University of Connecticut is largely supported by the NSF (Grant BIR9318373).

* Correspondence should be addressed to this author. Telephone: (908) 740-3429. FAX: (908) 740-4844. E-mail: william.windsor@spcorp.com.

‡ Schering-Plough Research Institute.

§ The University of Connecticut.

|| Present address: SmithKline Beecham Pharmaceuticals, R & D Bioinformatics, Mail Code UW2230, 709 Swedeland Rd., P.O. Box 1539, King of Prussia, PA 19406.

⊥ Present address: Alza Corp., 950 Page Mill Rd., Palo Alto, CA 94303-0802.

10.1021/bi981555y CCC: $15.00 © 1998 American Chemical Society
Published on Web 11/07/1998

recombinant muIL-10 (rmuIL-10) and recombinant huIL-10 (rhuIL-10) have a high α-helical content (∼60%), based on far-UV CD studies, suggests that the structure of IL-10 is similar to that of the four-α-helical bundle cytokine superfamily (*13*). The expression and purification of rmuIL-10 or rhuIL-10 from either *E. coli* or mammalian derived cells produce a species which has a size-exclusion chromatography elution profile consistent with that of a dimer (*6, 14*). The recently determined three-dimensional structure of rhuIL-10 (*17, 18*) confirmed that the protein is a homodimer and has a structural topology similar to the highly helical human gamma interferon molecule (*19, 20*).

The biological and structural stability of IL-10 is not well understood though the activity of the protein is known to be acid labile (*4*) and is biologically inactive following reduction of its two disulfide bonds (*13, 21*). A full biochemical and physicochemical characterization of the stability for rhuIL-10 is important in view of its many potential therapeutic uses. In this report we demonstrate that rhuIL-10 is a homodimer under our experimental conditions using several different techniques including chemical cross-linking, size-exclusion chromatography, and analytical ultracentrifugation. In addition, we describe our results regarding the stability of the protein as a noncovalent homodimer with respect to changes in pH, temperature, and increasing concentrations of guanidine hydrochloride. These unfolding studies revealed that while a soluble and highly structured monomer intermediate is obtained under denaturing conditions the biological activity of rhuIL-10 correlated only with the amount of dimer in solution. The observation of a stable monomer upon the dissociation of an oligomer is not a common event, thus, rhuIL-10 will be an important system for studying the mechanism of refolding and association of oligomers. Generation of a highly helical and soluble monomer was unexpected since molecular modeling analysis of the homodimeric three-dimensional structure indicated that two hydrophobic helices from each monomer are interwound into the other subunit and exposure of these hydrophobic regions to solvent would be thermodynamically and structurally unfavorable (*17, 18*). That the dimer state of rhuIL-10 appears to be the active species is consistent with the recent observation (*22*) that the extracellular domain of the recombinant human IL-10 receptor when bound to IL-10 forms a complex containing the equivalent of two IL-10 homodimers and four receptor monomers. In addition, by analogy to γ-interferon, recent modeling studies suggest a single IL-10 dimer could bind two receptors (*23*). The following report describes structure−function stability studies performed with rhuIL-10.

## MATERIALS AND METHODS

*Materials.* Recombinant huIL-10 derived from Chinese hamster ovary (CHO) cells was purified to greater than 95% by conventional chromatography (Biotechnology Bioisolation Group, Schering-Plough Research Institute). The chemical cross-linker reagent bis(sulfosuccinimidyl) suberate ($BS_3$) and guanidine hydrochloride (GndHCl) were obtained from Pierce. All protein concentrations were determined spectroscopically using a molar extinction coefficient of 8740 $M^{-1}$ $cm^{-1}$ ($\epsilon^{0.1\%} = 0.47$ $mg^{-1}$ $cm^2$) at 280 nm (*13*).

*Analytical Ultracentrifugation.* A sample of rhuIL-10 (∼1 mg/mL) was dialyzed against a 20 mM Tris buffer at pH 8 containing 0.15 M NaCl. In a typical experiment, 100 μL of the sample solution was loaded into one of the three solution channels of the 12 mm six channel exterior loading analytical ultracentrifuge cell (*24*) which was equipped with sapphire windows and interference masks. Dilutions to ∼0.1 and 0.3 mg/mL of the original sample were made with the dialysate and placed into the other two channels. The solution channels were previously filled with 10 μL of fluorocarbon oil (Minnesota Mining and Manufacturing Co., #FC-43) in order to make the bottom of the solution visible. One hundred and twenty microliters of the dialysate buffer was loaded into each of the solvent channels. The cell was centrifuged at 4 °C in a Beckman Model E analytical ultracentrifuge at 18k rpm overnight.

The data were acquired through a real time TV system which records the fringe displacement as a function of distance from the center of rotation with a typical error of about ±0.01−0.02 fringes (*25*). Under these conditions, this corresponds to a concentration error of ±3−6 μg/mL. Data were taken every 2−4 h in order to test for equilibrium. Equilibrium was determined when no change in the gradient was observed after subtracting successive interferograms from each other. Equilibrium was achieved overnight. Following data acquisition at equilibrium, the centrifuge was accelerated to 24k rpm, and equilibrium data were recorded following another overnight run. Blank runs ($H_2O$ vs $H_2O$) were performed under the identical conditions as the sample runs and subtracted from the final equilibrium data to correct for optical distortions.

Data analysis was performed using a nonlinear least-squares program (*26*) to fit all of the data globally. In addition to the ideal single-species model, this program allows the testing of various self-association models. The program yields a value of sigma [$\sigma = W^2M(1 - \bar{v})/RT$] for either the single nonideal species or that of the smallest associating species and the model of self-association with the smallest association constant. The criteria for goodness of fit required the rms error to be < 0.02 fringes (∼6 μg/mL) and nonsystematic.

To convert values of sigma into molecular weight, the specific volume ($\bar{v}$) and the density are needed. The former was calculated as 0.735 mL/g from the amino acid composition (*27*). The density of the solvent was estimated from density tables to be 1.006 g/mL at 4 °C.

*pH and GndHCl-Dependent Chemical Cross-Linking.* pH-dependent cross-linking was performed with 0.33 mg/mL samples and equilibrated in the following 40 mM buffers for 1 h at room temperature: sodium citrate (pH 2.0−3.6), sodium acetate (pH 4.2−5.7), sodium phosphate (pH 6.3), Hepes (pH 6.6, 7.0), sodium bicarbonate (pH 8.0−10.0). These samples were neutralized to pH 8.5 by diluting the sample 2-fold using 0.4 M sodium bicarbonate and then cross-linked immediately with 1 mM $BS_3$ for 30 min at room temperature. Samples were also cross-linked following treatment with GndHCl. RhuIL-10 samples, at 0.35 mg/mL, were incubated for 30 min with 0−6 M GndHCl in 50 mM sodium bicarbonate, pH 8.5, at room temperature prior to cross-linking with 1 mM $BS_3$ for 30 min at room temperature. Both the pH and GndHCl cross-linking reactions were stopped using 0.1 M TRIS, pH 8.5, and analyzed under reducing conditions by SDS−PAGE. The GndHCl-treated samples were dialyzed against 0.1% acetic acid,

lyophilized, and resuspended in SDS sample buffer prior to SDS−PAGE. Control experiments demonstrated that high concentrations of GndHCl did not interfere in the cross-linking reaction (data not shown).

*MC/9 Biological Assay: pH-Dependent Stability.* The biological activity of rhuIL-10 was determined using the murine mast cell proliferation (MC/9) assay costimulated with murine interleukin 4 (*1*). The pH-dependent biological stability of rhuIL-10 was determined by first preincubating a 0.1 mg/mL sample in 16 different pH buffers (see below) for 24 h at either 4 or −20 °C followed by a 1000-fold dilution into the assay media which was sufficient for analysis of its biological activity and to neutralize the pH of the sample.

*Far-UV CD pH and GndHCl Structural Stability Studies.* The pH-dependent structural stability of rhuIL-10 was measured by analyzing changes in the far-UV CD spectrum of the protein under different pH conditions. A stock solution at 0.5−0.7 mg/mL in 10 mM sodium phosphate, pH 7.0, was diluted 10-fold into the following solutions containing a final concentration of 20 mM buffer and 50 mM potassium sulfate: sodium citrate pH 2.5−3.5, sodium acetate pH 4.0−5.25, sodium phosphate pH 5.5−6.5, Hepes pH 7.0 and 7.5, and TRIS pH 8.0−10.0 (pH measurements were recorded following each experiment). Samples were equilibrated for 30 min at room temperature prior to measurement (unfolding was found to be complete within 1 min following a pH change). Refolding of the pH 2.5 sodium citrate equilibrated sample was achieved by diluting the sample 10-fold into a 20 mM Hepes, pH 7.0, buffer, equilibrated for 1 h at room temperature followed by the far-UV CD measurement. The percent unfolding was determined by measuring the change in ellipticity at 222 nm for each pH with respect to the ellipticity at pH 6.5. Nonlinear least-squares analysis was used to determine the p$K_a$ assuming the reaction underwent a two-state transition.

The GndHCl-dependent unfolding of rhuIL-10 was performed by diluting a 0.5−0.7 mg/mL sample 10-fold into a solution containing increasing concentrations of GndHCl. The final buffer composition and protein concentration were 50 mM TRIS, pH 8.5, 0−7.3 M GndHCl, and 0.05−0.07 mg/mL, respectively. Samples were equilibrated for 30 min at room temperature (22 °C) prior to measurement. The percent unfolding was determined by measuring the change in ellipticity at 222 nm for each GndHCl condition with respect to the total ellipticity change between 0 and 7 M GndHCl. A 6.2 M GndHCl-treated sample (0.77 mg/mL) was refolded by diluting the sample 10-fold to produce a GndHCl concentration of 0.62 M, which in the far-UV CD unfolding studies did not induce a conformational change.

The free energy change of unfolding, $\Delta G_D^{H2O}$, for $\gamma$-IFN was determined assuming a two-state unfolding mechanism, $N_2 \rightleftharpoons 2U$ (*28*). Under this condition, the equilibrium constant, $K_U$, is expressed as $K_U = [U]^2/[N_2] = 2P_t[f_U/f_M] = 2P_t[f_U^2/(1 - f_U)]$, where $f_U$ and $f_N$ represent the fractions of protein present in the unfolded (U) and native folded (N) states of the monomer, respectively, and $P_t$ is the total protein concentration (monomer units). Calculation of the free energy of unfolding is obtained from the equation: $\Delta G_D = -RT \ln (K_U)$. The values for $f_U$ and $f_N$ were determined using pre- and post-transition base lines as suggested by Santoro and Bolen (1988) (*29*). The following equation presented by Greene and Pace (1974) (*30*) was used to estimate the free energy of unfolding in water, $\Delta G_D^{H2O}$:

$$\Delta G_D = \Delta G_D^{H2O} - m[\text{GndHCl}] \quad (1)$$

where *m*, the slope of the curve, indicates the ability of a denaturant to unfold a protein and [GndHCl] is the concentration of denaturant. Calculations of $\Delta G_D^{H2O}$ were performed using $\Delta G_D$ values between ±1.2 kcal/mol of the $\Delta G_D$ value at $[\text{GndHCl}]_{1/2}$ to minimize extrapolation errors (*31*), where $[\text{GndHCl}]_{1/2}$ is the concentration of GndHCl at 50% unfolding.

Far-UV CD studies were recorded using an IBM-interfaced Jasco 500C spectropolarimeter. Spectra were recorded using a 0.1 cm cell for sample concentrations between 0.03 and 0.08 mg/mL, and each sample spectrum had a solvent spectrum subtracted from it. Each spectrum was averaged from 4−8 scans at a rate of 20 nm/min using a time constant of 1 s. The spectropolarimeter was calibrated using ammonium *d*-10-camphorsulfonate (Aldrich, Milwaukee, WI) (*32*, *33*).

## RESULTS AND DISCUSSION

*Analysis of Aggregation State.* The aggregation state of CHO-derived rhuIL-10 was examined using SDS polyacrylamide gel electrophoresis (SDS−PAGE) with and without chemical cross-linking, size-exclusion chromatography, and analytical ultracentrifugation. The apparent molecular mass ($M_{app}$) of rhuIL-10 determined by SDS−PAGE under reducing (Figure 1) and nonreducing conditions (data not shown) was ∼18 and 17 kDa, respectively. These results were consistent with the predicted molecular mass of 18 647 Da. The smaller apparent size for the nonreduced sample was most likely due to structural constraints produced by the two intramolecular disulfide bonds in rhuIL-10 (*13*). Electrospray mass spectroscopy analysis of rhuIL-10 indicated the protein had an *m*/*z* value of 18 643 (data not shown) and is the mass expected for native rhuIL-10 which contains two disulfide bonds (less four hydrogen atoms). CHO-derived rhuIL-10 has a potential N-glycosylation site at residue Asn116, however, the mass spectroscopy results strongly suggested that it was not glycosylated.

Chemical cross-linking of rhuIL-10 using $BS_3$ in a buffer equilibrated at pH 8.5 produced a species that migrated in SDS−PAGE with an apparent molecular mass consistent with that of a dimer, ∼36 kDa, Figure 1. In addition, size-exclusion chromatography of native and acid- or temperature-induced denatured rhuIL-10 produced two different elution peaks corresponding to dimer and monomer species, respectively (data not shown).

Finally, sedimentation equilibrium ultracentrifugation studies were performed to confirm the dimer state of rhuIL10. Five data sets were analyzed consisting of 1540 data points covering a range of concentrations from ∼3 $\mu$g/mL (0.08 $\mu$M dimer) to ∼2 mg/mL (54 $\mu$M dimer) at 4 °C. The best fit of the data, shown in Figure 2, indicated rhuIL-10 is a dimer with a molecular mass of 39.8 ± 0.4 kDa (RMS = 3.4 $\mu$g/mL) and weakly associates to tetramer. A value of $\bar{v}$ 2.3% less than that calculated for the protein could have lead to the 6.7% overestimate of the molecular mass actually measured. Analysis of the data using a monomer−dimer

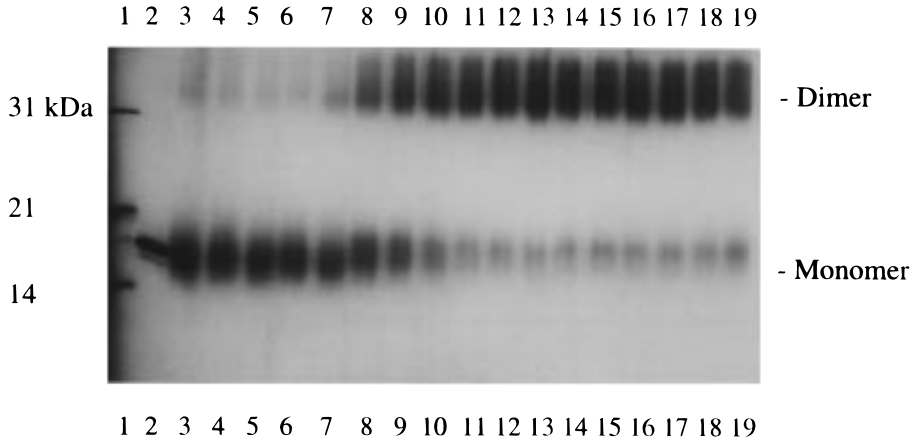


FIGURE 1: SDS−PAGE reducing gel: pH-dependent cross-linking of rhuIL-10. Lane 1, molecular mass standards; lane 2, rhuIL-10 control (no cross-linking); lanes 3−19 contain rhuIL-10 equilibrated into the following pH, neutralized, and cross-linked with $BS_3$: pH 2.0, 2.6, 3.1, 3.6, 4.2, 4.4, 4.6, 4.8, 5.1, 5.3, 5.7, 6.3, 6.6, 7.0, 8.0, 9.0, 10. Lane 1 contains a minor unknown contaminant running just below the IL-10 band. The gel was run with 1 $\mu$g of rhuIL-10 per lane and silver stained.

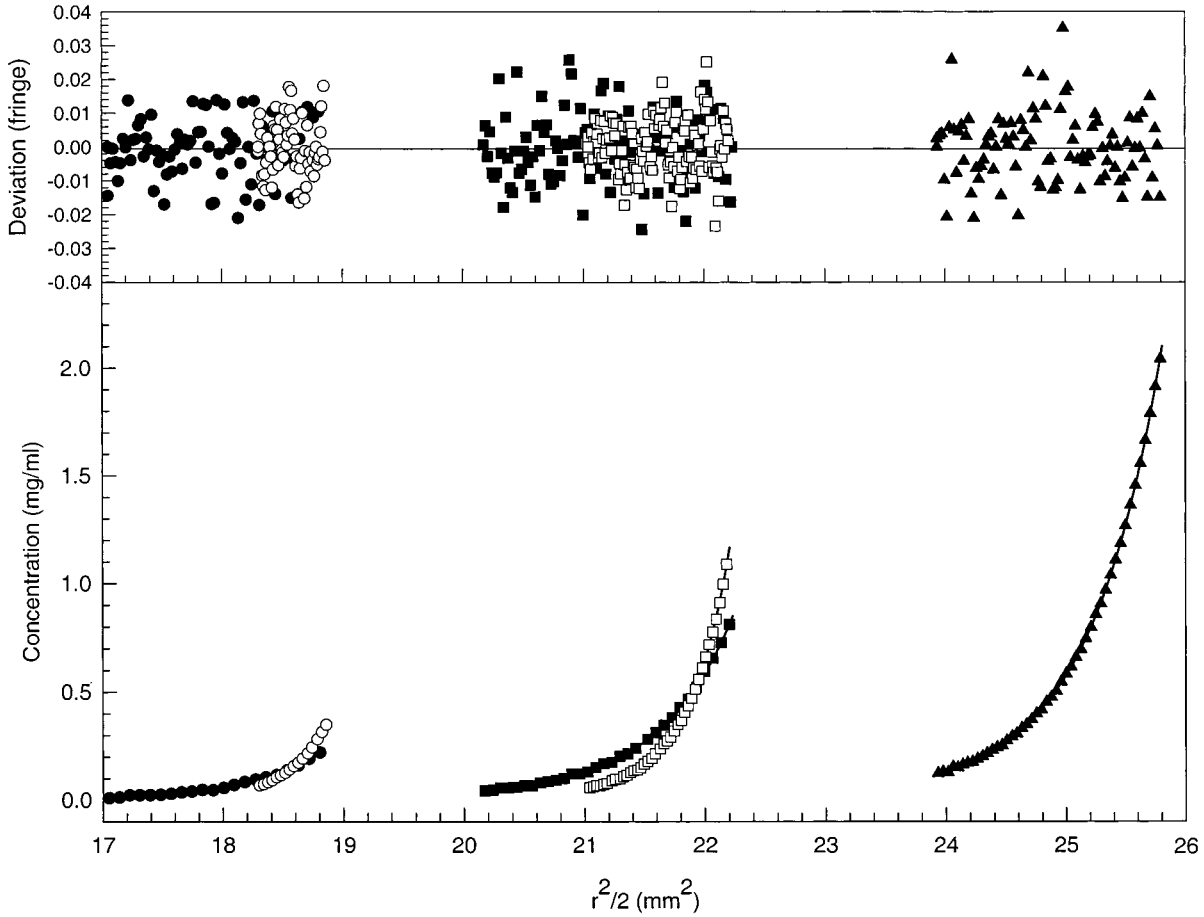


FIGURE 2: Equilibrium sedimentation of rhuIL-10 at 4 °C. The equilibrium data were fit using a nonlinear least-squares analysis (*26*); see text. Loading concentrations, 0.1 (circles), 0.3 (squares), and 1 mg/mL (triangles). Two different sedimentation speeds were performed for each sample: 15k rpm (closed symbols) and 25k rpm (open symbols). The buffer was 20 mM Tris, pH 8.0, containing 0.15 M NaCl.

equilibrium indicated that under our experimental conditions there was no detectable monomer species (< 3 $\mu$g/mL or 0.08 $\mu$M dimer at 4 °C). The weak dimer−tetramer association constant ranged from 0.03 to 0.5 $M^{-1}$ and indicated that ~6% tetramer is present at 2 mg/mL (54 $\mu$M dimer).

These ultracentrifugation results as well as the SDS−PAGE cross-linking, mass spectroscopy, and size-exclusion chromatography studies indicate CHO-derived rhuIL-10 exists in solution as a noncovalent homodimer under the protein concentrations and buffer conditions used in these experiments. In addition, the protein does not appear to be glycosylated. The dimer aggregation state of rhuIL-10 is similar to other α-helical cytokines such as IL-5, M-CSF, and $\gamma$-IFN, although $\gamma$-IFN is the only noncovalent dimer whose three-dimensional structure is similar to rhuIL-10.

*pH-Dependent Biological and Structural Stability.* We also examined the biological and structural stability of rhuIL-

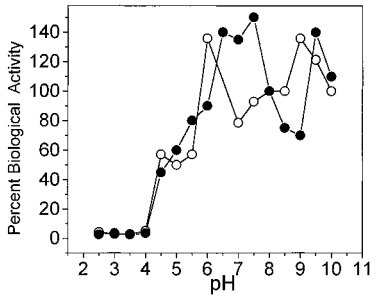


FIGURE 3: pH-dependent MC/9 biological activity. RhuIL-10 was preincubated at each pH for 24 h followed by a 1000-fold dilution into the assay media to neutralize the sample. During the preincubation, the samples were either stored at 4 °C (open circles) or frozen at −20 °C (solid circles). The percent activities are relative to a nontreated standard.

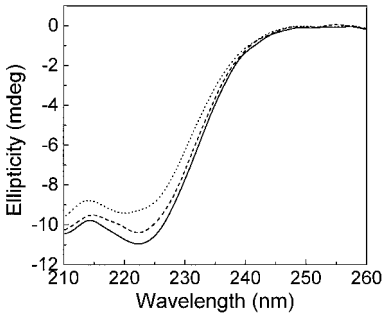


FIGURE 4: Far-UV circular dichroism. (—) RhuIL-10 control at pH 7.0; (•••) rhuIL-10 at pH 2.5; (- - -) rhuIL-10 neutralized from pH 2.5 to pH 7.0. The pH 7.0 samples were in 20 mM Hepes, 50 mM potassium sulfate, and the pH 2.5 sample was in 20 mM sodium citrate, 50 mM potassium sulfate.

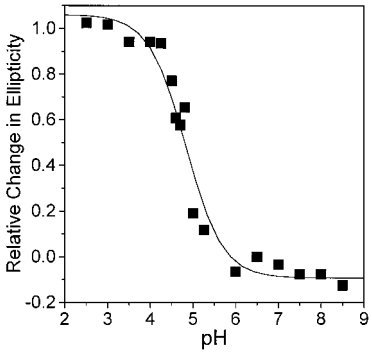


FIGURE 5: Relative pH-dependent changes in the far-UV CD. RhuIL-10 was incubated at each pH for 30 min, 22 °C, and the ellipticity was measured at 222 nm. A p$K_a$ of 4.8 ± 0.1 was calculated assuming a single two-state unfolding transition.

10 with respect to pH. The protein has an unusually neutral isoelectric point (p*I*) compared to most lymphokines. The predicted p*I* is 7.5 and is similar to the experimentally determined p*I* of ∼7.88 using isoelectric focusing electrophoresis (*21*). The pH-dependent stability of the rhuIL-10 MC/9 biological activity was determined by diluting rhuIL-10 stock solutions to 0.1 mg/mL in 16 different buffers adjusted to pH values between 2.5 and 10 and equilibrated for ∼24 h at either 4 or −20 °C. These samples were then diluted 1000-fold into assay media and tested for biological activity. The pH-dependent activity of rhuIL-10 at 4 °C (Figure 3) demonstrated that the protein retained high activity between pH 6 and 10. However, below pH 6.0 the activity decreased significantly such that at pH 2.5 only a small percent activity remained. Samples stored for 24 h at −20 °C had a similar pH-dependent activity profile. The pH value at which there was 50% biological activity (p$K_a^{MC/9}$) occurred at approximately pH 4.8. The lack of activity for the acid-treated samples suggested that rhuIL-10 could not sufficiently renature to its native state under the conditions employed in this experiment (diluted to 0.1 μg/mL and neutralization to pH 7.0 with assay media and frozen until assayed).

Since rhuIL-10 is a noncovalent dimer, we decided to examine the aggregation state of the protein with respect to pH using chemical cross-linking and SDS−PAGE analysis and compare the degree of dimer formation to the pH-dependent biological activity of the protein. A major advantage of this technique is that even though pH-induced denaturation would result in large insoluble aggregates, all of the rhuIL-10 species would be detected due to the solubilizing effect of SDS. Samples equilibrated at room temperature for 1 h in different pH buffers were subsequently adjusted to pH 8.5, chemically cross-linked with $BS_3$, and analyzed by SDS−PAGE under reducing conditions. Figure 1 shows the relative mobility of each pH-treated and cross-linked sample. Samples equilibrated at a pH between 5.1 and 10.0 migrated with a $M_{app}$ ∼36 kDa, consistent with a dimer aggregation state. The small amount of monomer present in these experiments may have been generated from some $BS_3$ lysine-modified samples which induced dimer dissociation. Covalent modification of lysine residues by $BS_3$ is also likely to have caused the bandwidths of the chemically modified samples to be significantly wider than the non-cross-linked samples.

Samples equilibrated in buffers below pH 5.1 contained increasing amounts of monomer and a concomitant decrease in the amount of dimer such that samples between pH 2.0 and 3.6 appeared to exist primarily as monomer (Figure 1). Based on the intensities of the monomer and dimer bands, the pH at which there was approximately 50% dissociation, p$K_a^{BS3-pH}$, was between 4.6 and 4.8. RhuIL-10 was also observed to be a monomer at pH 2.0 by FPLC size-exclusion chromatography (data not shown).

In a previous report, we determined from an analysis of the CHO-derived rhuIL-10 far-UV CD spectrum that the protein contained ∼60% α helix (*13*). The high helical content has since been confirmed by X-ray crystallography to be approximately 67% (*17*, *18*). To determine the structural stability of this α-helical protein, we measured the change in ellipticity at 222 nm with respect to changes in pH. Decreases in the ellipticity at 222 nm indicated the protein underwent a conformational change upon lowering the pH from 7.0 to 2.5 (Figure 4). The calculated midpoint or apparent p$K_a$ for the pH-induced unfolding (apparent p$K_a^{CD-pH}$), assuming a two state transition, was 4.8 ± 0.1 (Figure 5). This acidic apparent p$K_a^{CD-pH}$ value for the pH-induced unfolding of rhuIL-10 correlated directly with the MC/9 biological assay p$K_a^{MC/9}$ value, ∼4.8, as well as the chemical cross-linking dimer dissociation p$K_a^{BS3-pH}$ value, 4.6−4.8. Thus, rhuIL-10 appears to undergo a pH-induced conformational change which promotes subunit dissociation below pH 5.5. The corresponding loss of MC/9 biological activity with decreasing pH suggests that the dimer is the active species.

Though low-pH conditions induced conformational changes, the ellipticity value at 222 nm for the pH 2.5 treated sample

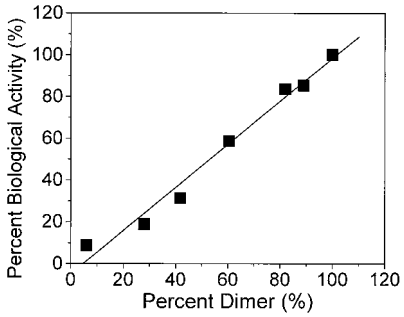


FIGURE 6: Relative MC/9 biological activity with respect to the percent rhuIL-10 dimer. RhuIl-10 at 0.1 mg/mL was heated to 55 °C for 1−10 min to induce dimer dissociation. The relative amount of dimer formed following heating was determined by size-exclusion chromatography (24 mL Superdex 75 column, 40 mM Hepes, pH 7, 0.2 M NaCl) at 4 °C. The percent dimer was calculated based on the area of the dimer for each heated sample and compared to an unheated control. The MC/9 biological activity was determined from the same heated sample used for size-exclusion chromatography, and the relative activities were based on comparisons to an unheated sample. A linear least-squares fit of the data resulted in a slope of 1.03, an intercept of −4.9, and a correlation coefficient of 0.98.

decreased by only 11% compared to the pH 7.0 sample (Figure 4) and the shape retained minima at 208 and 222 nm. This suggested that the rhuIL-10 monomer retained a high degree of α-helical structure even at pH 2.5. It is not known whether the tertiary state of the monomer at pH 2.5 is similar to that in the native dimer conformation or to that of a molten globular state containing a high degree of α-helical secondary structure. It is also possible that some of the α helicity seen at pH 2.5 is due to constraints resulting from the presence of two disulfide bonds (*13*) which inhibit full unfolding.

In refolding studies, a pH 2.5 sample neutralized to pH 7.0 and equilibrated for 1 h had a final ellipticity value, at 222 nm, that was 96.4% of the control sample and suggested that partial refolding occurred (Figure 4). Subsequent size-exclusion chromatography analysis showed that the residual incomplete refolding was likely to be due to the incomplete reassociation of the monomer species which was present at only 8%.

*Temperature-Dependent Dimer Dissociation.* Temperature-dependent stability studies of the rhuIL-10 dimer dissociation process were also performed. Using size-exclusion chromatography as a monitoring technique, it was observed that a 0.3 mg/mL (8 $\mu$M dimer) protein sample equilibrated for 1 h, at temperatures of 37 and 55 °C, resulted in the formation of 2% and 22% monomeric species, respectively (data not shown). Moreover, this temperature-induced dimer dissociation process exhibited a strong dependence on the concentration of the protein in the sample. As an illustration, a similar treatment for a 0.05 mg/mL (1.3 $\mu$M dimer) sample resulted in the formation of 10% and 55% monomeric species in the equilibrated mixture when heated at 37 and 55 °C, respectively.

The relationship between the temperature-induced subunit dissociation and MC/9 biological activity of rhuIL-10 was also determined. Samples were heated to 55 °C for 1−10 min, and the percent dimer was determined from the area recorded by size-exclusion chromatography. A fraction of each heated sample loaded onto the column was also assayed for MC/9 activity. These samples were diluted 1000-fold prior to assay. The linear dependence of the MC/9 activity with respect to the percent dimer shown in Figure 6 demonstrates the important role the rhuIL-10 dimer has in promoting the biological response.

*GndHCl-Dependent Dimer Dissociation and Structural Stability.* We have also examined dimer dissociation and unfolding of rhuIL-10 with respect to increasing concentrations of GndHCl to provide additional information regarding the general structural stability properties of the protein and to enable comparisons of its stability to other dimer systems. GndHCl-induced dimer dissociation of rhuIL-10 was determined initially by chemical cross-linking using $BS_3$ in the presence of increasing concentrations of GndHCl, at pH 8.5, followed by analysis of the amounts of monomer and dimer in each solution by SDS−PAGE (following dialysis). The results of this study, presented in Figure 7, demonstrated that dimer dissociation was complete using only ∼1.6 M GndHCl and 50% dissociation ($[GndHCl]_{1/2}$) occurred with ∼0.75−0.9 M GndHCl (controls were performed to confirm that GndHCl did not interfere with $BS_3$ cross-linking). These results have been confirmed using size-exclusion chromatography. The value for $[GndHCl]_{1/2}$ is relatively low compared to values reported for many other homo- and heterodimers (*28, 34, 35*) and suggested that the stability of the rhuIL-10 dimer to denaturants was relatively weak perhaps due to different subunit intermolecular interactions such as electrostatic interactions (see below).

In several previously reported dimer dissociation systems, GndHCl- or urea-induced dissociation followed a two-state

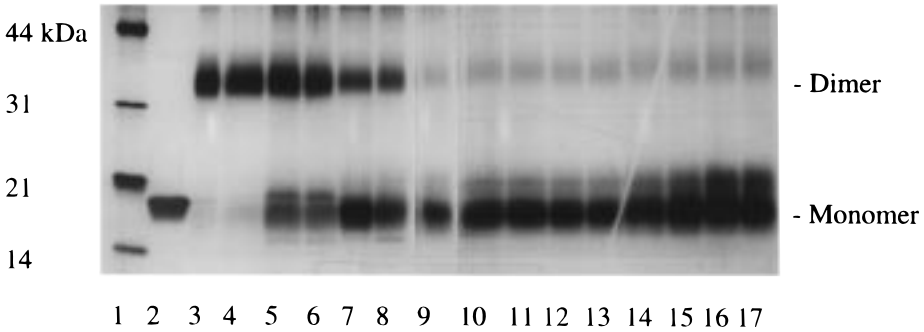


FIGURE 7: SDS−PAGE analysis of the GndHCl-dependent dissociation of rhuIL-10. RhuIL-10 was incubated with 0−6 M GndHCl in 50 mM sodium bicarbonate, pH 8.5, for 30 min, 22 °C, cross-linked with $BS_3$, dialyzed, and analyzed using silver-stained reducing SDS−PAGE (see Materials and Methods). Lane 1: molecular mass standards; lane 2, rhuIL-10 control (non-cross-linked); lanes 3−17, GndHCl concentrations 0, 0.25, 0.5, 0.75, 0.9, 1.0, 1.6, 2.0, 2.5, 3.0, 3.5, 4.0, 4.5, 5.0, 6.0.

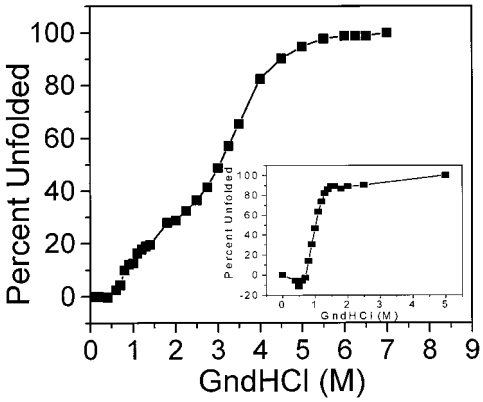


FIGURE 8: Far-UV CD GndHCl-dependent unfolding of rhuIL-10. RhuIL-10 (0.05−0.07 mg/mL) was incubated with 0−7.3 M GndHCl, 50 mM TRIS, pH 8.5, for 30 min at 22 °C prior to measuring the ellipticity at 222 nm. The relative percent unfolding was determined using 0 and 7.3 M GndHCl as the folded and unfolded end points, respectively. Insert: Far-UV CD GndHCl-dependent unfolding of $\gamma$-IFN. The sample concentration and buffer composition are the same as used for rhuIL-10.

dissociation process, $N_2 \leftrightarrow 2U$, where N is the native monomer conformation and U is the unfolded monomer conformation (*28*, *34*−*39*). These unfolding studies were performed by measuring conformationally sensitive spectroscopic properties such as fluorescence or CD. To further examine the stability properties and unfolding pathway of rhuIL-10, we performed far-UV CD measurements in the presence of increasing concentrations of GndHCl. GndHCl-induced conformational changes of rhuIL-10 were detected by measuring the relative change in ellipticity at 222 nm, and the unfolding profile, shown in Figure 8, was biphasic with respect to increasing concentration of GndHCl. The first unfolding phase (phase I) occurred between 0.6 and ∼1.4 M GndHCl and accounted for an ∼20% change in the total unfolding process. Based on the GndHCl $BS_3$ cross-linking studies, it appeared that phase I corresponded to conformational changes correlated with the dissociation of the rhuIL-10 dimer to separate monomers. These cross-linking studies also suggested that the inflection for phase I seen at ∼1 M GndHCl corresponded to the point in which the rhuIL-10 dimer was almost fully dissociated to monomers (also confirmed by size-exclusion chromatography, data not shown). Thus, phase I appeared to reflect a simple two-state dissociation reaction, $N_2 \leftrightarrow 2I$, where I is the conformation of a dissociated monomer with a high helical content and more structurally stable than the fully unfolded monomer, U, observed at 5.5−7.3 M GndHCl.

The second unfolding phase (phase II) extended over a much greater concentration range of GndHCl, 1.4−5.5 M, where concentrations above 5.5 M GndHCl represented the fully unfolded state. Since phase II occurred under conditions where only rhuIL-10 monomer existed, this phase apparently described the unfolding of the individual subunits, $2I \leftrightarrow 2U$, and reflected the structural stability of the rhuIL-10 monomer. The shallow monomer unfolding curve seen in phase II for rhuIL-10 is similar to that seen for several cytokine monomers such as IL-4 and GM-CSF which are 4-α-helical bundles and contain 3 and 2 disulfide bonds, respectively (*33*). Together, phases I and II of rhuIL-10 appear to represent the entire unfolding reaction (Scheme 1).

Scheme 1

$$N_2 \leftrightarrow 2I \leftrightarrow 2U$$

To determine the free energies of unfolding for both of these coupled reactions, a series of protein concentration-dependent unfolding studies similar to that describe by Clark et al. (1993) (*36*), Neet and Timm (1994) (*28*), and Grimsley et al. (1997) (*39*) should be performed.

Since the three-dimensional structure of rhuIL-10 is similar to the $\gamma$-IFN homodimer, we performed a similar GndHCl unfolding study on human $\gamma$-IFN to determine if these structurally related proteins had similar stability properties. In contrast to rhuIL-10, the unfolding profile of $\gamma$-IFN had a single, very sharp, unfolding phase, similar to a two-state unfolding reaction, with a $[GndHCl]_{1/2}$ value of 0.95 M, Figure 8 (insert). The values of the free energy of unfolding, $\Delta G_D^{H2O}$, for a two-state dimer unfolding reaction, $N_2 \leftrightarrow 2U$, are usually between 10 and 30 kcal/mol (*28*) where the lower values indicate dimers more readily unfold and dissociate to the unfolded monomer state. Analysis of this curve according to a two-state dimer dissociation reaction, $N_2 \leftrightarrow 2U$ (see Materials and Methods), gave values for $\Delta G_D^{H2O}$ and $m$ of 12.5 kcal mol$^{-1}$ and 5.7 kcal mol$^{-1}$ M$^{-1}$, respectively (*28*). The unfolding profile of $\gamma$-IFN was similar to the dimer dissociation process seen in phase I for rhuIL-10, however, the absence of a second phase suggested that the $\gamma$-IFN monomer was not as structurally stable.

*Structural Analysis of RhuIl-10: Stability Properties.* The observed apparent p$K_a$ values (∼4.8) for loss in biological activity, structural unfolding, and subunit dissociation suggest that protonation of the 21 aspartic and glutamic acid residues and the subsequent potential loss of stabilizing interactions such as H-bonds, ionic interactions, and salt bridges under acidic conditions promote subunit dissociation. We analyzed the three-dimensional structure of rhuIL-10 (*20*) to determine if there were unique structural reasons for the pH-induced subunit dissociation and structural stability (high helical content) of the acid- or GndHC-induced rhuIL-10 monomer. The structure of rhuIL-10 contains two identical monomers with two helices from one monomer intercalated into four helices of the other monomer, and acidic residues comprise 8.2% of the dimer interface. These residues are distributed throughout the surface of the monomer−monomer interface along the E and F helices of one monomer and the A′, B′, and C′ helices of the second monomer. The acidic residues participate in a variety of hydrogen bonds and ion pairs (Table 1) and are likely to be important in stabilizing the dimer state above pH 4.5. The ion pair between glutamate 151 and arginine 27′ was noted as a possible stabilizing interaction in the determination of the rhuIL-10 X-ray structure (*17*). Under partial denaturation conditions, a highly helical monomer intermediate, I, was observed. This observation is contrary to modeling studies by Zdanov et al. (1995) (*17*), who concluded that in order for a monomer, containing six α helices, to exist in a conformation identical to one side of the 2-fold symmetric dimer that either the Cys62−Cys114 disulfide would have to be reduced or the structure would have to be seriously distorted. Neither disulfide bond is broken in rhuIL-10, however, the far-UV CD for the monomer intermediate, I, does undergo an ∼20% change. This suggests that the protein may indeed undergo

Table 1: Acidic Residues and Ion Pairs Buried on IL-10 Dimer Association

| acidic residue monomer I (region) | ion pair residue monomer II (region) | surface area buried (Å$^2$) |
|---|---|---|
| Asp 41 (helix A) | Tyr 137′ backbone (helix F′) | 42.2 |
| Asp 55 (helix B) | Ser 118′ backbone (helix E′) | 37.3 |
| Glu 67 (helix C) | Lys 117′, Lys 125′ (helix E′) | 84.4 |
| Glu 75 (helix C) | Lys 125′ (helix E′) | 31.8 |
| Glu 142 (helix F) | Leu 48′ backbone (helix B′) Lys 138 (helix F) | 73.3 |
| Asp 144 (helix F) | Lys 34′, Gln 38′ (helix A′) | 40.6 |
| Glu 151 (helix F) | Arg 27′ (helix A′) | 59.3 |
| total acidic area/monomer | | 368.9 |
| total acidic area/dimer | | 737.8 |

a conformational rearrangement sufficient to achieve a structure with helical content resembling that of the six-helical bundle.

$\gamma$-IFN (*19*) is structurally similar to rhuIL-10, but the structural stability of the $\gamma$-IFN monomer appears to be less than the rhuIL-10 monomer. The enhanced stability of the rhuIL-10 monomer may be due to the presence of two intramolecular disulfide bonds in rhuIL-10 and none in $\gamma$-IFN. Stability differences may also be facilitated due to differences in the amount and type of surface area buried between each monomer. A significant difference in buried surface area exists between $\gamma$-IFN and rhuIL-10, 7628 and 8975 Å$^2$, respectively, however, the percent acidic residues buried for $\gamma$-IFN (7.9%) is similar to that of rhuIL-10 (8.2%).

## SUMMARY

The stability studies presented in this report indicate that the highly helical rhuIL-10 homodimers can be dissociated with pH, GndHCl, and temperature to form monomers which retain a high degree of α-helical secondary structure. Our temperature-dependent studies indicate rhuIL10 dimers, when heated to 37 °C for 1 h, undergo ∼10% subunit dissociation when low protein concentrations (<50 $\mu$g/mL) are used. Thus, in vivo conditions (low protein concentration and 37 °C) are likely to promote the conversion of a significant amount of IL-10 dimer to monomers. Our biological assay results, however, suggest that only the dimer species is biologically active since the activities of solutions containing monomers were inactive. The formation of monomers by these perturbing methods may partially denature the monomer structure to an inactive state. There are structural reasons why the rhuIL-10 dimer is the active species. Recently, Walter et al. (1995) (*20*) reported the crystal structure of the $\gamma$-IFN/$\gamma$-IFN receptor complex. The homodimer of $\gamma$-IFN is bound by two $\gamma$-IFN receptors in a 2-fold symmetry which is consistent with the known role of cytokines for inducing the aggregation of two or more cell surface receptors from which signal transduction is generated. This model is also appropriate for rhuIL-10 which has a similar dimer structure to $\gamma$-IFN and the IL-10 receptor belongs to the same class II hematopoietic receptor super family. Based on these structural similarities, Zdanov et al. (1996) (*23*) were successful in generating a three-dimensional computer model of a complex between a dimer of IL-10 and two IL-10 receptor monomers that showed excellent complementarity for both polar and hydrophobic interactions within the proposed binding contact regions. In addition, Tan et al. (1995) (*22*) have recently reported that when the recombinant IL-10 extracellular domain receptor is bound to IL-10 the complex formed is consistent with two IL-10 dimers and four receptor monomers. For these reasons, it is likely that the biologically relevant state of rhuIL-10 is as a dimer.

That the IL-10 monomer shows a high amount of α-helical content suggests it may retain some of the native conformation. Provided with the three-dimensional structure of the rhuIL-10 dimer, one may be able to redesign the protein to obtain a more stable monomer which may retain receptor binding activity but lack biological activity due to the failure to induce the association of cell surface receptors. The antagonist activity of this type of protein may be therapeutically valuable. Investigations of the structure/function properties of the rhuIL-10 monomer are currently underway.

## REFERENCES


1. O'Garra, A., Stapelton, G., Dhar, V., Pearce, M., Schumacher, J., Rugo, H., Barbis, D., Stall, A., Cupp, J., Moore, K., Vieira, P., Mosmann, T., Whitmore, A., Arnold, L., Haughton, G., and Howard, M. (1990*) Int. Immunol. 2,* 821−832.
2. Suda, T., O'Garra, A., MacNeil, I., Fisher, M., Bond, M. W., and Zlotnik, A. (1990) *Cell. Immunol. 129,* 228−240.
3. de Wall-Malefyt, R., Abrams, J., Bennett, B., Figdor, C. G., and de Vries, J. E. (1991*) J. Exp. Med. 174,* 1209−1220.
4. Fiorentino, D. F., Bond, M. W., and Mosmann, T. R. (1989*) J. Exp. Med. 170,* 2081−2095.
5. Howard, M., O'Garra, A., Ishida, H., de Wall Malefyt, R., and de Vries, J. (1992) *J. Clin. Immunol. 12,* 239−247.
6. Moore, K. W., O'Garra, A., de Wall Malefyt, R., Vieira, P., and Mosmann, T. (1993) *Annu. Rev. Immunol. 11,* 165−190.
7. Pennline, K. J., Roque-Gaffney, E., and Monahan, M. (1994*) Clin. Immunol. Imunopathol. 71,* 169−175.
8. Willems, F., Marchant, A., Delville, J. P., Gerard, C., Delvaux, A., Velu, T., de Boer, M., and Goldman, M. (1994) *Eur. J. Immunol. 24,* 1007−1009.
9. Marchant, A., Bruyns, C., Vandenabeele, P., Ducarme, M., Gerard, C., Delvaux, A., DeGroote, D., Abramowicz, D., Velu, T., and Goldman, M. (1994) *Eur. J. Immunol. 24,* 1167−1171.
10. Katsikis, P. D., Chu, C. Q., Brennan, F. M., Maini, R. N., and Feldman, M. (1994) *J. Exp. Med. 179,* 1517−1527.
11. Moore, K. W., Vieiram P., Fiorentino, D. F., Trounstine, M. L., Khan, T. A., and Mosmann, T. R. (1990) *Science 248,* 1230−1234.
12. Vieira, P., de Wall-Malefyt, R., Dang, M.-N., Johnson, K. E., Kastelein, R., Fiorentino, D. F., deVries, J. E., Roncarolo, M.-G., Mosmann, T. R., and Moore, K. W. (1991*) Proc. Natl. Acad. Sci. U.S.A. 88,* 1172−1176.
13. Windsor, W. T., Syto, R., Tsarbopoulos, A., Zhang, R., Durkin, J., Baldwin, S., Paliwal, S., Mui, P. W., Pramanik, B., Trotta, P. P., and Tindall, S. H. (1993) *Biochemistry 32,* 8807−8815.
14. Tan, J., Indelicato, S. R., Narula, S. K., Zavodny, P. J., and Chou, C.-C. (1993*) J. Biol. Chem. 268,* 21053−21059.
15. Ho, A. S. Y., Liu, Y., Khan, T. A., Hsu, D.-H., Bazan, J. F., and Moore, K. W. (1993) *Proc. Natl. Acad. Sci. U.S.A. 90,* 11267−11271.
16. Bazan, J. F. (1990) *Proc. Natl. Acad. Sci. U.S.A. 87,* 6934−6838.
17. Zdanov, A., Schalk-Hihi, C., Gutshina, A., Tsang, M., Weatherbee, J., and Wlodawer, A. (1995) *Structure 3,* 591−601.
18. Walter, M., and Nagabhushan, T. (1995) *Biochemistry 34,* 12118−12125.
19. Ealick, S. E., Cook, W. J., Vijay-Kumar, S., Carson, M., Nagabhushan, T. L., Trotta, P. P., and Bugg, C. E. (1991) *Science 252,* 698−702.
20. Walter, M., Windsor, W., Nagabhushan, T., Lundell, D., Lunn, C., Zavodny, P., and Narula, S. (1995) *Nature 376,* 230−235.
21. Trotta, P., and Windsor, W. (1995) *Interleukin-10, Molecular Biology Intelligence Unit* (deVries, J. E., and de Wall Malefyt, R., Eds.) pp 11−18, Landes Publishing Co., Austin, TX.

22. Tan, J., Braun, S., Rong, H., DiGiacomo, R., Dolphin, E., Baldwin, S., Narula, S., Zavodny, P., and Chou, C. (1995) *J. Biol. Chem. 270,* 12906−12911.
23. Zdanov, A., Schalk-Hihi, C., and Wlodawer, A. (1996) *Protein Sci. 5,* 1955−1962.
24. Ansevin, A. T., Roark, D., and Yphantis, D. A. (1970) *Anal. Biochem. 34,* 237−261.
25. Laue, T. M., Yphantis, D. A., and Rhodes D. G. (1984) *Anal. Biochem. 143,* 103−116.
26. Johnson, M. L., Correia, J., Yphantis, D. A., and Halvorson, H. R. (1981) *Biophys. J. 36,* 575−588.
27. Cohn, E. J., and Edsall, J. T., Eds. (1943) *Proteins, Amino Acids, and Peptides*, pp 370−381, Reinhold Publishing Corp., New York.
28. Neet, K., and Timm D. (1994) *Protein Sci. 3,* 2167−2174.
29. Santoro, M., and Bolen, D. (1988) *Biochemistry 27,* 8063−8068.
30. Greene, R., and Pace, C. N. (1974) *J. Biol. Chem. 240,* 5388−5393.
31. Pace, C. N. (1986) *Methods Enzymol. 131,* 266−280.
32. Takakuwa, T., Konno, T., and Meguro, H. (1985) *Anal. Sci. 1,* 215−218.
33. Windsor, W., Syto, R., Le, H., and Trotta, P. (1991) *Biochemistry 30,* 1259−1264.
34. Timm, D., and Neet, K. (1992*) Protein Sci. 1,* 236−244.
35. Liang, H., Sandberg, W., and Terwilliger, T. (1993) *Proc. Natl. Acad. Sci. U.S.A. 90,* 7010−7014.
36. Clark, A. C., Sinclair, J., and Baldwin, T. O. (1993) *J. Biol. Chem. 268,* 10773−10779.
37. Milla, M., and Sauer, R. (1995) *Biochemistry 34,* 3344−3351.
38. Gloss, L., and Matthews, C. R. (1997) *Biochemistry 36,* 5612−5623.
39. Grimsley, J., Scholtz, J., Pace, C. N., and Wild, J., (1997) *Biochemistry 36,* 14366−14374.

BI981555Y